Inorganic Chemistry

Communication

pubs.acs.org/IC

Structure and Dynamics of Dodecaborate Clusters in Water

Khadga Karki,[†] Detlef Gabel,[†,‡] and Danilo Roccatano*,[†]

[†]School of Engineering and Science, Jacobs University Bremen, Campus Ring 1, D-28759 Bremen, Germany

[‡]Department of Chemistry, University of Bremen, D-28334 Bremen, Germany

Supporting Information

ABSTRACT: We have studied using molecular dynamics simulations the interaction of the dodecaborate anion, $B_{12}H_{12}^{2-}$, and its amino, trimethyl, and triethyl derivatives with water molecules. We found peculiar organization of the water molecules in the first solvation shell with the formation of a dihydrogen bond between the hydrogen atoms of the anions and the hydrogen atoms of the water molecules. The simulations also show that the organization of the hydration shell is strongly influenced by the substituents in the anions. These differences are likely to play an important role in understanding the interaction of the anions with biological systems like membranes and proteins in aqueous environments.

The dodecaborate cluster $B_{12}H_{12}^{2-}$ and its derivatives are weakly coordinating ions that have found use, among others, in boron neutron capture therapy,[1,2] as ionic liquids,[3] and in molecular imaging with the prospect of using nonlinear optical spectroscopy.[4] Derivatives of the dodecaborate cluster have been known to bind to lipid membranes and influence their structure and tightness,[5,6] and they, as well as other boron cluster compounds, also act as enzyme inhibitors.[7−10] The nature of the interaction of boron clusters with biological interfaces, either lipid bilayers or protein surfaces, has not yet been understood. In addition, the structure of the hydration shell of these anions in water has so far not been studied in detail. To the best of our knowledge, only a few experimental studies using IR spectroscopy have pointed out the presence of a peculiar dihydrogen bond between the boron hydrogen atoms of the anions and the hydrogen of proton donors such as methanol.[11−13]

To shed light on the nature of these processes, new molecular models for molecular dynamics (MD) simulations of a series of boron cluster anions have been derived. The models are optimized against experimental water/1-octanol partition coefficient data[7] (see details in the Supporting Information, SI) such that they can be used to investigate interaction of the molecules with biological interfaces like lipid layers. Here, we present the results of the MD simulations done in water that provide evidence for the peculiar hydration-shell structures, showing dihydrogen bonds between the anions and water molecules. The simulations also show that the orientation of the water molecules around the anions is influenced by the substituents.

In the $B_{12}H_{12}^{2-}$ anion (Figure 1a), the delocalized three-center, two-electron bonding,[14] also labeled as three-dimensional aromaticity,[15] imparts a rather peculiar charge distribution: the peripheral hydrogen atoms have partial negative charges, while the inner boron atoms have partial positive charges (see the SI for the table of partial charges). This contrasts with the charge distribution in aromatic systems such as benzene, in which the outer hydrogen atoms have partial positive charges while the inner carbon atoms have partial negative charges. Because the anion is centrosymmetric (I_h symmetry), it does not possess a dipole moment. Functionalization with an amino group[16] leads to singly charged $B_{12}H_{11}NH_3^-$ (Figure 1b); with this substitution, the dipole moment increases drastically to about 11 D because of the asymmetric structure and inhomogeneous charge distribution. The nitrogen atom in the amino group has a significant partial negative charge of about −0.79 eu, while the *N*-bonded hydrogen atoms have partial positive charges of about 0.36 eu. The hydrogen atoms bonded to the boron atoms have net negative charges, but the charge distribution among them is not uniform; the hydrogen atoms on the belt shaded with green in Figure 1 are less negative than the hydrogen atoms on the belt shaded with yellow. Correspondingly, the boron atoms on the first belt are negatively charged, while those on the second belt are positively charged. Functionalization to trimethyl (Figure 1c) and triethyl (Figure 1d) groups changes the overall charge distribution, thereby increasing the dipole moment to about 14 and 18 D, respectively, with similar patterns of charge distribution.

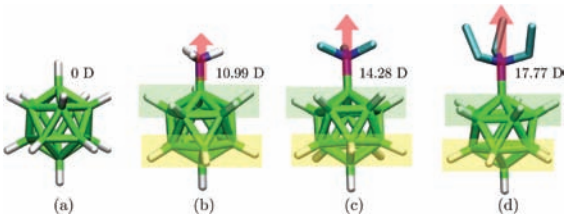

Figure 1. Optimized geometries of (a) dodecaborate and (b) ammonio-, (c) trimethylammonio-, and (d) triethylammoniododecaborates. The arrows indicate the direction and size of the dipole moments. Green-shaded hydrogen atoms are less negatively charged than the yellow-shaded hydrogen atoms.

The water−octanol partition coefficient was calculated from the solvation free energies (see details in SI). The free energies obtained from the simulations are given in Table 1. The table also shows the partition coefficient log *P* obtained from the simulations and experiments. The calculated values are consistent and in close agreement with the experimental data.

Received: February 2, 2012
Published: April 9, 2012

   dx.doi.org/10.1021/ic300223z | *Inorg. Chem.* 2012, 51, 4894−4896

Table 1. Solvation Free Energies (in kJ/mol) and Partition Coefficients

	$B_{12}H_{11}N(CH_3)_3$	$B_{12}H_{11}N(C_2H_3)_3$
$\Delta_{water}G$	615 ± 1	587 ± 1
$\Delta_{oct}G$	602 ± 2	582 ± 2
$\Delta_{vac}G$	86.03 ± 0.01	76.99 ± 0.1
$\Delta_{hyd}G$	−529 ± 1	−510 ± 1
$\Delta_{solv}G$	−516 ± 2	−505 ± 2
log P_{OW}	−2.3 ± 0.5	−0.87 ± 0.5
log P_{OW} (exp.)	−1.4 ± 0.1	−0.48 ± 0.02

Functionalization affects interaction of the anions with the water molecules. The pair correlation functions $g_{x,y}(r)$ at distance r between a virtual particle x placed at the center of mass of the anions and the oxygen atoms of water y are shown in Figure 2a. The potential of mean force (PMF) $w(r)$[17]

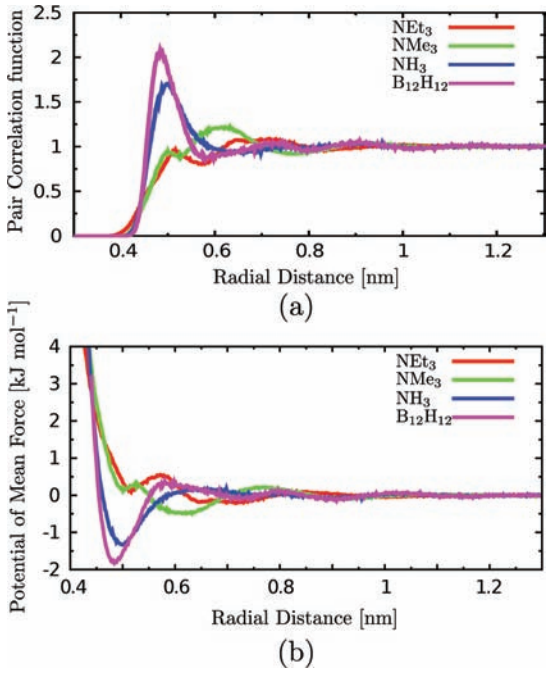

Figure 2. Pair correlation function between a virtual particle placed at the center of mass of the anions and the oxygen atoms (a) and the PMF of the interaction of oxygen atoms of water with the anions (b).

computed using the relation $g_{x,y}(r) = \exp[-w(r)/kT]$, where k is Boltzmann's constant and T is the simulation temperature, gives progressively decreasing interaction energies of 1.81, 1.34, 0.48, and 0.2 kJ mol^{-1} for unfunctionalized dodecaborate and amino-, trimethyl- and triethyl-functionalized anions, respectively (Figure 2b). This trend in the interaction energies follows the experimentally observed solubility of the anions in water: the unfunctionalized anion is the most soluble, and the triethyl-functionalized anion is the least soluble.

The geometry of the first solvation shell in all of the anions is anisotropic, as can be seen in the spatial distribution function (SDF; Figure 3) of hydrogen and oxygen atoms of water around the anions. The distributions in the unfunctionalized anion show concentric rings on top of the hydrogen atoms of the anions.

The most probable distance between the hydrogen atoms of water molecules in the first hydration shell and the anion is 0.16 nm, which is substantially shorter than 0.24 nm corresponding

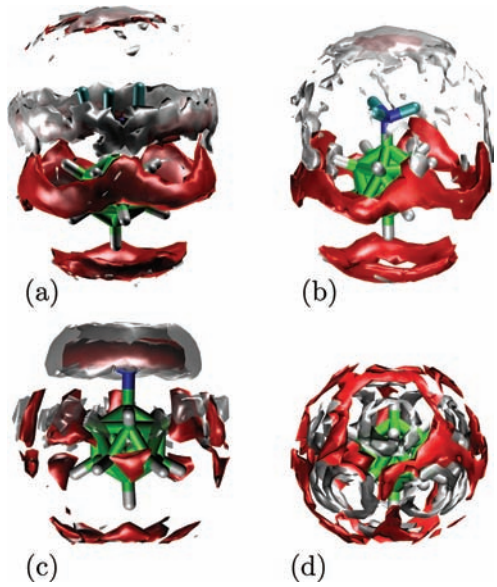

Figure 3. SDFs of the hydrogen and oxygen atoms of water around the boron anions: (a) ethyl-, (b) methyl-, and (c) amino-funtionalized and (d) unfunctionalized. Gray and red isosurfaces represent the distribution of the hydrogen and oxygen atoms, respectively. Isosurfaces have been chosen to distinctly show the first solvation shell.

to twice the van der Waals radius of a hydrogen atom (H−H and H−O pair correlation functions corresponding to the SDFs are shown in Figure 5 of SI). The distance observed in the model is consistent with the proposed O−H···H−B dihydrogen bond[18] distance in various molecules. Two types of hydrogen bonds are observed (Figure 4). They involve (case A in Figure

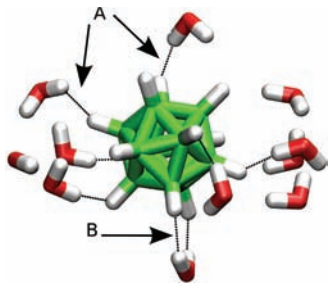

Figure 4. Snapshot from simulations showing some of the water molecules around the $B_{12}H_{12}^{2-}$ cluster forming two types (A and B) of O−H···H−B dihydrogen bonds.

4) one or both of the hydrogen atoms (case B in Figure 4) of a single water molecule. The average number of water molecules in the first shell is ≈22 for $B_{12}H_{12}^{2-}$ and ≈18 for the substituted anions. The average number of water molecules forming bridged O−H···H−B dihydrogen bonds are ≈10 for $B_{12}H_{12}^{2-}$ and ≈6 for the other anions.

The most probable distance between the oxygen atoms of the water molecules in the first hydration shell and the hydrogen atoms of the anion is 0.26 nm; the SDFs show preferential orientation of the water molecules around the boron cluster, with the hydrogen atoms of the water molecules pointing toward the cluster and the oxygen atoms pointing away. In amino- and ethyl-functionalized anions, the solvent molecules form an annular density distribution around the functional group; here the orientation of the water molecules is

dx.doi.org/10.1021/ic300223z | Inorg. Chem. 2012, 51, 4894−4896

reversed; the oxygen atoms point toward the functional groups, while the hydrogen atoms point away, as shown in Figure 3c. The distribution reflects the partial charges in the functional groups; the positively charged hydrogen atoms of the amino group and the carbon atoms attached to the nitrogen atoms in the ethyl group attract the negatively charged oxygen atoms of the water molecules. Such an annular density distribution is not present around the methyl group because the carbon atoms in the group have very small partial charges. The density of the hydrogen and oxygen atoms above the methyl and ethyl groups, with the oxygen atoms distributed at the center, is due to the orientation of the solvent molecules induced by the strong dipole moment of the anions. Such a cap, although present, is not conspicuous above the unsubstituted ammonio group.

The dynamic properties of the anions also vary with the functional groups. The translational diffusion coefficients of the anions computed using the relation $6Dt = \lim_{t\to\infty} \langle |\mathbf{r}_i(t) - \mathbf{r}_i(0)|^2 \rangle$, where D is the diffusion coefficient, $\mathbf{r}_i(t)$ is the coordinate of the anion at time t, and $\mathbf{r}_i(0)$ is the coordinate at time $t = 0$,[19,20] are $(1.6 \pm 0.1) \times 10^{-9}$, $(1.4 \pm 0.1) \times 10^{-9}$, $(1.3 \pm 0.1) \times 10^{-9}$, and $(1.8 \pm 0.2) \times 10^{-9}$ m^2 s^{-1} for the ethyl-, methyl-, and amino-functionalized and unfunctionalized anions, respectively. The diffusion coefficients do not follow the usual mass relation derived from the Einstein–Stokes relation[21] $D \propto m^{-1/3}$ (here m is the mass of the molecule), which shows that the diffusion is affected by the solvation shell around the molecules.

The effect of the geometry of the solvation shell can also be observed in the rotational motion of the anions. The dipole correlation function is related to the rotational time constant[20]

$$C_2(t) = \langle P_2[\mu(0)\,\mu(t)] \rangle = A \exp(-t/\tau_2) \qquad (2)$$

where P_2 is the second-order Legendre polynomial, μ is the dipole moment, A is a normalization constant, and τ_2 is the rotational time constant; the subscript 2 is used to emphasize that the second-order Legendre polynomial is used to compute the correlation. The correlation functions calculated from the simulations give rotational time constants of 16.76 ± 0.09, 10.48 ± 0.04, and 14.62 ± 0.05 ps for ethyl-, methyl-, and amino-functionalized anions, respectively.

In summary, we have developed force-field parameters for the MD simulations of the unfunctionalized and ammonio-, trimethylammonio-, and triethylammonio-functionalized dodecaborate clusters. MD simulations of the clusters in water show that water distributes quite differently around the anions and that the orientation depends strongly on the substituents of the cluster. The solvation shell around the molecule also affects the dynamics of the molecules. The differences in the distribution of the solvation shell as well as the dynamics of the molecules might play an important role in the interaction of the molecules with biological systems such as lipid membranes and proteins in aqueous environments.

■ ASSOCIATED CONTENT

Supporting Information

Details of the computational methods and calculations of the partition coefficients of $B_{12}H_{11}N(CH_3)_3$ and $B_{12}H_{11}N(C_2H_5)_3$, coordinates of the atoms of the optimized structures of $B_{12}H_{12}^{2-}$, $B_{12}H_{11}NH_3$, $B_{12}H_{11}N(CH_3)_3$, and $B_{12}H_{11}N(C_2H_5)_3$, and all parameters for the anion force field. This material is available free of charge via the Internet at http://pubs.acs.org.

■ AUTHOR INFORMATION

Corresponding Author

*E-mail: d.roccatano@jacobs-university.de.

Notes

The authors declare no competing financial interest.

■ ACKNOWLEDGMENTS

This study was performed using the computational resources of the HLRN (Computer Laboratories for Animation, Modeling and Visualization). This work was performed within the graduate program "Nanomolecular Science" at Jacobs University Bremen.

■ REFERENCES

(1) Kageji, T.; Nagahiro, S.; Kitamura, K.; Nakagawa, Y.; Hatanaka, H.; Haritz, D.; Grochulla, F.; Haselsberger, K.; Gabel, D. *Int. J. Radiat. Oncol.* **2001**, *51*, 120–130.

(2) Soloway, A. H.; Tjarks, W.; Barnum, B. A.; Rong, F.-G.; Barth, R. F.; Codogni, I. M.; Wilson, J. G. *Chem. Rev.* **1998**, *98*, 1515–1562.

(3) Justus, E.; Rischka, M.; Wishart, J. F.; Werner, K.; Gabel, D. *Chem.—Eur. J.* **2008**, *14*, 1918–1923.

(4) Nicoud, J.-F.; Bolze, F.; Sun, X.-H.; Hayek, A.; Baldeck, P. *Inorg. Chem.* **2011**, *50*, 4272–4278.

(5) Awad, D.; Damian, L.; Winterhalter, M.; Karlsson, G.; Edwards, K.; Gabel, D. *Chem. Phys. Lipids* **2009**, *157*, 78–85.

(6) Schaffran, T.; Li, J.; Karlsson, G.; Edwards, K.; Winterhalter, M.; Gabel, D. *Chem. Phys. Lipids* **2010**, *163*, 64–73.

(7) Schaffran, T.; Justus, E.; Elfert, M.; Chen, T.; Gabel, D. *Green Chem.* **2009**, *11*, 1458–1464.

(8) Cigler, P.; Kozisek, M.; Rezacova, P.; Brynda, J.; Otwinowski, Z.; Pokorna, J.; Plesek, J.; Grüner, B.; Doleckova-Maresova, L.; Masa, M.; Sedlacek, J.; Bodem, J.; Krausslich, H. G.; Kral, V.; Konvalinka, J. *Proc. Natl. Acad. Sci. U.S.A.* **2005**, *102*, 15394–15399.

(9) Rezacova, P.; Pokorna, J.; Brynda, J.; Kozisek, M.; Cigler, P.; Lepsik, M.; Fanfrlik, J.; Rezac, J.; Saskova, K. G.; Sieglova, I.; Plesek, J.; Sicha, V.; Grüner, B.; Obersinkler, H.; Sedlacek, J.; Krausslich, H. G.; Hobza, P.; Kral, V.; Konvalinka, J. *J. Med. Chem.* **2009**, *52*, 7132–7141.

(10) Scholz, J.; Blobaum, A. L.; Marnett, L. J.; Hey-Hawkins, E. *Bioorg. Med. Chem.* **2011**, *19*, 3242–3248.

(11) Filipov, O. A.; Filin, A. M.; Teplitskaya, L. N.; Belkova, N. V.; Shmyrova, Y. V.; Sivaev, I. B.; Bregadze, V. I.; Epstein, L. M.; Shubina, E. S. *Main Group Chem.* **2005**, *4*, 97–110.

(12) Shubina, E. S.; Bakhmutova, E. V.; Filin, A. M.; Sivaev, I. B.; Teplitskaya, L. N.; Christyakov, A. L.; Stankevich, I. V.; Bakhmutov, V. I.; Epstein, L. M. *J. Organomet. Chem.* **2002**, *657*, 155–162.

(13) Fanfrlik, J.; Lepsik, M.; Horinek, D.; Havlas, Z.; Hobza, P. *ChemPhysChem* **2006**, *7*, 1100–1105.

(14) Williams, R. E. *Chem. Rev.* **1992**, *92*, 177–207.

(15) King, R. B. *Chem. Rev.* **2001**, *101*, 1119–1152.

(16) Hertler, W.; Raasch, M. S. *J. Am. Chem. Soc.* **1964**, *86*, 3661–3668.

(17) Chandler, D. *Introduction to modern statistical mechanics*; Oxford University Press: Oxford, U.K., 1987; Chapter 7, p 201.

(18) Custelcean, R.; Jackson, J. E. *Chem. Rev.* **2001**, *101*, 1963–1980.

(19) Allen, M. P.; Tildesley, D. J. *Computer Simulation of Liquids*; Clarendon Press: Oxford U.K., 1991.

(20) Karki, K.; Roccatano, D. *J. Chem. Theory Comput.* **2011**, *7*, 1131–1140.

(21) Karki, K.; Materny, A.; Roccatano, D. *Phys. Chem. Chem. Phys.* **2011**, *13*, 11864–11871.